

# DuetGraph: Coarse-to-Fine Knowledge Graph Reasoning with Dual-Pathway Global-Local Fusion

Jin Li<sup>1,3,†</sup>, Zezhong Ding<sup>2,3,†</sup>, Xike Xie<sup>1,3\*</sup>

<sup>1</sup>School of Biomedical Engineering, University of Science and Technology of China (USTC)

<sup>2</sup>School of Artificial Intelligence and Data Science, USTC

<sup>3</sup>Data Darkness Lab, Suzhou Institute for Advanced Research, USTC

{lijinstu, zezhongding}@mail.ustc.edu.cn, xkxie@ustc.edu.cn

## Abstract

Knowledge graphs (KGs) are vital for enabling knowledge reasoning across various domains. Recent KG reasoning methods that integrate both global and local information have achieved promising results. However, existing methods often suffer from score over-smoothing, which blurs the distinction between correct and incorrect answers and hinders reasoning effectiveness. To address this, we propose DuetGraph, a *coarse-to-fine* KG reasoning mechanism with *dual-pathway* global-local fusion. DuetGraph tackles over-smoothing by segregating—rather than stacking—the processing of local (via message passing) and global (via attention) information into two distinct pathways, preventing mutual interference and preserving representational discrimination. In addition, DuetGraph introduces a *coarse-to-fine* optimization, which partitions entities into high- and low-score subsets. This strategy narrows the candidate space and sharpens the score gap between the two subsets, which alleviates over-smoothing and enhances inference quality. Extensive experiments on various datasets demonstrate that DuetGraph achieves state-of-the-art (SOTA) performance, with up to an **8.7%** improvement in reasoning quality and a **1.8×** acceleration in training efficiency.

## 1 Introduction

Knowledge graphs (KGs) are structured representations of real-world entities and their relationships, widely applied in domains such as information retrieval [1, 2], recommendation systems [3, 4], materials science [5, 6], and biomedical research [7, 8]. However, existing KGs are often incomplete, missing certain factual information [9, 10], which limits their effectiveness in downstream applications. As a result, inferring and completing missing entity information through KG reasoning is essential.

KG reasoning faces two fundamental challenges. Firstly, it requires effective aggregation and propagation of local neighborhood information to capture multi-hop and subgraph patterns among entities. Secondly, it must capture global structure and long-range dependencies across large-scale graphs to understand complex relationships that span multiple intermediate nodes. To address these challenges, a substantial line of previous research has been dedicated to developing methods to capture local neighborhood and global structure for KG reasoning. These methods can be categorized into two types: *message passing-based methods* and *transformer-based methods*.

Message passing-based KG reasoning methods [11, 12, 3] effectively capture local structural information via message passing mechanism [13], but often fail to model long-range dependencies and global structural patterns [14, 15]. In contrast, transformer-based KG reasoning methods excel at capturing global KG information and long-range dependencies but tend to overlook important local structures

\*Corresponding Author    †Equal Contribution

or short-range dependencies between neighboring entities [16]. To address these limitations, recent state-of-the-art (SOTA) studies [17, 18] have shifted to integrate both local and global information by stacking message-passing networks and attention layers in a single stage.

However, such a single stage stacking approach tends to result in the problem of score **over-smoothing**, where incorrect answers receive scores similar to correct ones (Figure 1<sup>2</sup>), making them hard to distinguish. Accordingly, we summarize the problem into two core challenges. **Challenge 1:** Existing studies [21, 22] have shown that stacking either message-passing or attention layers individually deepens information propagation and aggravates the over-smoothing problem. When message-passing and attention layers are stacked together, these effects accumulate. **Challenge 2:** The discriminative capacity of single stage models is typically limited [23], as they generate the answer directly based on a one-shot reasoning. This deficiency in discrimination further exacerbates the over-smoothing phenomenon [24].

To address these challenges, we propose **DuetGraph**, a coarse-to-fine KG reasoning mechanism with dual-pathway global-local fusion. To address **Challenge 1**, we propose a dual-pathway fusion model (Section 3.1) that separately processes global and local information before adaptively fusing them. By segregating message-passing and attention layers, rather than stacking them, our model alleviates over-smoothing and improves reasoning quality. For **Challenge 2**, we propose the coarse-to-fine reasoning optimization (Section 3.2), which first employs a coarse model to predict and partition candidate entities into high- and low-score subsets, and then applies a fine model to predict the final answer based on the subsets. It enhances robustness against over-smoothing and improves reasoning quality. We theoretically demonstrate the effectiveness of coarse-to-fine optimization by mitigating over-smoothing in Section 3.2. Furthermore, we demonstrate the effectiveness of this optimization in improving inference in Section 4.4.

Our contributions can be summarized as follows. **1)** We propose DuetGraph, a novel KG reasoning framework to alleviate score over-smoothing in KG reasoning. Specifically, DuetGraph: a) utilizes a dual-pathway fusion of local and global information instead of a single-pathway method, and b) adopts a coarse-to-fine design rather than one stage design. **2)** We theoretically demonstrate that our proposed dual-pathway reasoning model and coarse-to-fine optimization can both alleviate over-smoothing, thus effectively enhancing inference quality. **3)** DuetGraph achieves SOTA performance on both inductive and transductive KG reasoning tasks, with up to an **8.7%** improvement in quality and a **1.8×** acceleration in training efficiency.

## 2 Background

**Knowledge Graph.** A knowledge graph (KG) is a structured representation of information where entities are represented as nodes, and the relationships between these entities are represented as edges. Typically, a KG  $\mathcal{G} = \{\mathcal{V}, \mathcal{E}, \mathcal{R}\}$  is composed of: a set of entities  $\mathcal{V}$ , a set of relations  $\mathcal{R}$ , and a set of triplets  $\mathcal{E} = \{(h_i, r_i, t_i) \mid h_i, t_i \in \mathcal{V}, r_i \in \mathcal{R}\}$ , where each triplet represents a directed edge  $h_i \xrightarrow{r_i} t_i$  between a head entity  $h_i$  and a tail entity  $t_i$ .

**Knowledge Graph Completion.** Given a KG  $\mathcal{G} = (\mathcal{V}, \mathcal{E}, \mathcal{R})$ , KG completion is to infer and predict missing elements within triplets to enrich the knowledge graph. Depending on the missing component, the task can be categorized into three subtypes: head entity completion  $(?, r, t)$ , tail entity completion  $(h, r, ?)$ , and relation completion  $(h, ?, t)$ . In this paper, we primarily focus on tail entity completion, following the setting of recent KG works [17, 18], as the other tasks can be reformulated into this one.

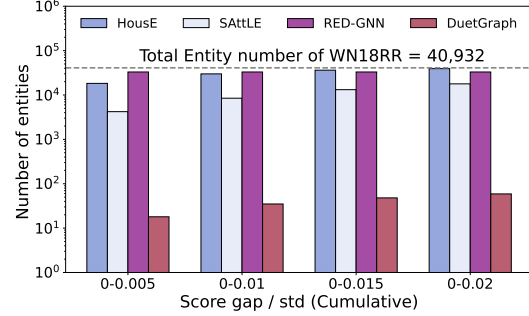


Figure 1: **Discriminative ability of KG reasoning models:** HousE [19], SAttLE [20], and RED-GNN [3] show limited discrimination, with many incorrect answers scoring close to the correct one. In contrast, our DuetGraph achieves clearer score separation, with far fewer incorrect answers near the correct score.

<sup>2</sup>The  $x$ -axis denotes normalized score gap  $(\frac{|\text{Score}_{\text{correct}} - \text{Score}_{\text{incorrect}}|}{\text{std}(\text{Score})})$  and  $y$ -axis indicates entity count per interval.

**Related Works.** KG reasoning methods can be classified based on their use of structural information: message passing-based methods, which primarily leverage local structures, and transformer-based methods, which mainly exploit global structures. Message passing-based methods, such as [3, 25, 26], suffer from well-known limitations of message-passing networks, including incompleteness [27] and over-squashing [28]. Transformer-based methods, such as [29, 30], also have drawbacks. For example, they typically transform graph structures into sequential representations during knowledge encoding, potentially losing critical structural information inherent to KGs [31]. Hybrid approaches that combine message-passing and transformers, such as [17, 18], leverage the strengths of both paradigms. However, they still face key challenges in effectively integrating and balancing local features learned via message passing with global KG information captured by self-attention. Besides, there are also triplet-based methods, such as TransE [32], ComplEx [33], DistMult [34], and RotatE [35], which treat triples as independent instances and often ignore graphs’ topological structure. Beyond these categories, other approaches include meta-learning methods like MetaSD [36], rule path-based models like RNNLogic [37], and tensor decomposition methods such as TuckER-IVR [38]. However, the optimization process of these methods does not directly take into account the issue of score over-smoothing. In response, we propose DuetGraph, explicitly addressing the challenge of score over-smoothing in KG reasoning.

### 3 DuetGraph

This section introduces DuetGraph, as shown in Figure 2<sup>3</sup>. The core architecture of DuetGraph consists of two components: a dual-pathway model for training (Steps ①-④), and a coarse-to-fine reasoning optimization for inference (Steps ⑤-⑧). Section 3.1 presents the dual-pathway global-local fusion model, and Section 3.2 details the coarse-to-fine reasoning optimization.

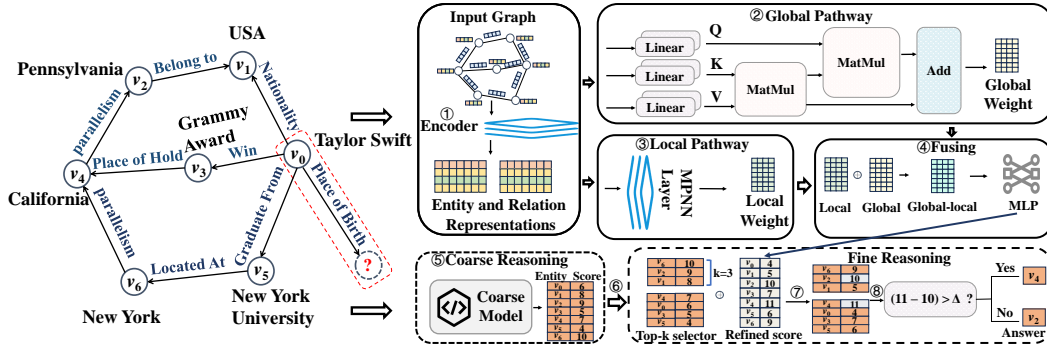


Figure 2: **Overview of DuetGraph:** ① Input KG to GNN encoder (e.g., GCN [13]) and output entity and relation representations; ② Employ a simple global attention mechanism [41] to compute the global weight; ③ Use the query-aware message passing networks [17] to compute the local weight; ④ Fuse the local and global weight using a multi-layer perceptron (MLP); ⑤ Use the coarse model (e.g., House [19] and RED-GNN [3]) to get the initial entity-to-score table; ⑥ Split the entity-to-score table into two subtables (i.e., high-score subtable and low-score subtable) based on Top- $k$  selector; ⑦ Update the two subtables based on the refined entity-to-score table predicted by dual-pathway global-local fusion model; ⑧ Output the answer based on the relationship between the maximum score gap of the two subsets and a predefined threshold  $\Delta$ .

<sup>3</sup>In dual-pathway model, after obtaining the representations in Step ④, we employ an MLP to transform each representation into a score. Loss function is defined for each training triplet  $(h, r, t)$ :  $\mathcal{L} = -\log(\sigma(t|h, r)) - \sum_{t'} \log(1 - \sigma(t'|h, r))$ , where  $\sigma(\cdot|h, r)$  denotes the score of a candidate triplet,  $t'$  denotes negative samples. Negative samples are generated by masking the correct answer and uniformly sampling with replacement from the remaining unmasked entities [39]. Finally, we update model parameters by optimizing negative sampling loss [35] with the Adam optimizer [40].

### 3.1 Dual-Pathway Global-Local Fusion Model

As previously mentioned, a single-pathway design is more likely to cause score over-smoothing, thereby impairing KG reasoning quality. Therefore, we decouple the message-passing networks and the transformer-based mechanism into two separate pathways, i.e., local pathway (Step ②) and global pathway (Step ③). Then, we fuse their outputs through an adaptive fusion model (Step ④). We detail the dual-pathway fusion model in the following paragraphs.

**Adaptive Global-Local Fusion.** A straightforward approach to achieve global-local information fusion is to simply sum the local and global weights. However, this method may fail to fully capture the complex interactions between local and global features, potentially hurting the model performance [42]. To address it, we introduce a learnable parameter  $\alpha$  to adaptively assign weights to local and global information, enabling a more effective weighted fusion of the two components. Therefore, the final entity representation matrix  $Z$  is computed as :

$$Z = \alpha \cdot Z_{\text{local}} + (1 - \alpha) \cdot Z_{\text{global}}, \quad (1)$$

where  $Z_{\text{local}}$  denotes the local weight matrix, obtained through local pathway (Step ②), and  $Z_{\text{global}}$  denotes the global weight matrix, obtained through global pathway (Step ③).

Then, the representation matrix  $Z$  can be used for predicting the entity scores by an MLP (Step ④).

**Theoretical Analysis.** Here, we theoretically show that our proposed dual-pathway fusion model offers superior alleviation of score over-smoothing compared to the single-pathway approach. To begin with, we give the upper bounds on entity score gap for both single-pathway and dual-pathway models in Lemma 1.

**Lemma 1 (Upper Bounds on Score Gap for Different Models).** *Let  $\mathcal{M}_O$  denotes the weight matrix [43] of single-pathway model stacked with message passing and transformer,  $\mathcal{M}_D$  denotes the weight matrix of our dual-pathway model. For any two entities  $u, v \in \mathcal{V}$ , the gap in their scores after  $\ell$  layers of iteration can be bounded by:*

$$|S_u - S_v| \leq 2L_f(\sigma_{\max}(\mathcal{M}))^\ell \|\mathbf{X}^{(0)}\|_2, \quad \mathcal{M} \in \{\mathcal{M}_O, \mathcal{M}_D\}, \quad (2)$$

where  $\sigma_{\max}(\mathcal{M})$  denotes the largest singular value of  $\mathcal{M}$ ,  $\mathbf{X}^{(0)}$  denotes initial entity feature matrix,  $L_f$  is the Lipschitz constant [44], and  $\|\cdot\|_2$  is Euclidean norm operation.

We provide a detailed proof of Lemma 1 in Appendix A.1. Based on Theorem 1, we theoretically establish the relationship between the score gap and the weight matrix for each respective model. Specifically, we can get that the upper bound on score gap is related to the largest singular value of the weight matrix  $\mathcal{M}$ . To further scale the inequality in Equation 2, we derive the largest singular value upper bound of the weight matrix in Lemma 2.

**Lemma 2 (Upper Bounds on Largest Singular Value).** *For a weight matrix  $\mathcal{M} \in \{\mathcal{M}_O, \mathcal{M}_D\}$ , its largest singular value satisfies*

$$\sigma_{\max}(\mathcal{M}) < 1. \quad (3)$$

We provide a detailed proof of Lemma 2 in Appendix A.1. Based on Lemmas 1 and 2, as the number  $\ell$  of iteration layers increases, the upper bound on score gaps **decrease exponentially** with respect to  $\sigma_{\max}(\mathcal{M})$  because of the exponential function's properties. A larger  $\sigma_{\max}(\mathcal{M})$  results in a greater upper bound and a slower decrease of it, suggesting that the model is more resistant to over-smoothing. Based on this, we further give the quantitative relationship between  $\sigma_{\max}(\mathcal{M}_O)$  and  $\sigma_{\max}(\mathcal{M}_D)$  in Lemma 3.

**Lemma 3 (Relationship between  $\sigma_{\max}(\mathcal{M}_O)$  and  $\sigma_{\max}(\mathcal{M}_D)$ ).** *Give the the learnable parameter  $\alpha$  in Equation 1, the relationship between  $\sigma_{\max}(\mathcal{M}_O)$  and  $\sigma_{\max}(\mathcal{M}_D)$  is:*

$$\sigma_{\max}(\mathcal{M}_D) > \alpha - (1 - \alpha)\sigma_{\max}(\mathcal{M}_O). \quad (4)$$

We provide a detailed proof of Lemma 3 in Appendix A.1. Based on Lemmas 1, 2, and 3, we can derive the relationship between the learnable parameter  $\alpha$  and the upper bound of the score gap, as shown in Theorem 1.

**Theorem 1 (Relationship between  $\alpha$  and Score Gap).** *If  $\alpha < \frac{\sigma_{\max}(\mathcal{M}_D) + \sigma_{\max}(\mathcal{M}_O)}{1 + \sigma_{\max}(\mathcal{M}_O)}$ , the score gap upper bound of the the dual-pathway model is greater than that of the single-pathway model and the dual-pathway model shows a slower decrease of the score gap upper bound.*

We provide a detailed proof of Theorem 1 in Appendix A.1. Our adaptive fusion approach drives  $\alpha$  below the theoretical threshold in Theorem 1 via parameter update with gradient descent. According to Theorem 1, the dual-pathway model outperforms the single-pathway model in mitigating over-smoothing.

**Complexity Analysis.** In this paragraph, we compare the time complexity of our dual-pathway fusion model with single-pathway approach. For a fair comparison, we assume both models have the same number of layers, including  $L_m$  message passing layers and  $L_t$  transformer layers. Under this setting, the overall time complexity of our dual-pathway fusion model and single-pathway approach is  $\mathcal{O}(\max(L_m(|\mathcal{E}|d + |\mathcal{V}|d^2), L_t|\mathcal{V}|d^2))$  and  $\mathcal{O}(L_m|\mathcal{E}|d + (L_m + L_t)|\mathcal{V}|d^2)$  respectively (we provide details in Appendix B.1.). Here,  $|\mathcal{V}|$  and  $|\mathcal{E}|$  respectively denote the number of entities and triplets and  $d$  is the dimension of entity representation. In single-pathway approach, the message passing and transformer run sequentially, so their time complexity add together. By contrast, our dual-pathway fusion model processes them in parallel, so the overall complexity is only determined by the more expensive pathway. As a result, the dual-pathway model yields better time efficiency.

### 3.2 Coarse-to-Fine Reasoning Optimization

To address the over-smoothing issue caused by the one-stage approach as discussed in Section 1, we decompose the KG reasoning into two sequential stages: coarse stage and fine stage, as shown in Steps ⑤, ⑥, ⑦, and ⑧. We detail the design and implementation of each stage in the following paragraphs.

**Stage 1: Coarse-grained Reasoning.** In this stage, we first obtain an entity-to-score table by using the coarse model (Step ⑤). Then, the table is split into two subtables based on their rankings (Step ⑥): a high-score subtable made up of the top- $k$  entities, and a low-score subtable containing the remaining ones. The formal description of this process is as follows. Given a query  $(h, r, ?)$ , let  $\mathcal{T} = \{(v, s_v) \mid v \in \mathcal{V}, s_v\}$  denote the full entity-to-score table, where  $s_v$  is the score of entity  $v$ .  $\text{Rank}(v)$  denotes the rank of entity  $v$  in descending order of the scores. Accordingly, we split  $\mathcal{T}$  into two subtables as follows:

$$\mathcal{T}^{\text{high}} = \{(v, s_v) \in \mathcal{T} : \text{Rank}(v) \leq k\}, \quad \mathcal{T}^{\text{low}} = \{(v, s_v) \in \mathcal{T} : \text{Rank}(v) > k\},$$

where  $k$  is a hyperparameter controlling the cutoff rank.  $\mathcal{T}^{\text{high}}$  is the high-score subtable and  $\mathcal{T}^{\text{low}}$  is the low-score subtable.

**Stage 2: Fine-grained Reasoning.** At this stage, we firstly update  $\mathcal{T}^{\text{high}}$  and  $\mathcal{T}^{\text{low}}$  with the fine model (i.e., the dual-pathway model introduced in Section 3). Then, we extract the entities with the highest score from each subtables, denoted as  $(e_h, s_{e_h})$  for  $\mathcal{T}^{\text{high}}$  and  $(e_l, s_{e_l})$  for  $\mathcal{T}^{\text{low}}$ . After that, we compute the difference  $\gamma = s_{e_l} - s_{e_h}$  based on the pre-defined threshold  $\Delta$ . If  $\gamma$  exceeds  $\Delta$ , this indicates that the highest-scoring entity in the low-score subtable clearly surpasses the highest-scoring entity in the high-score subtable. Therefore, we select the highest-scoring entity from  $\mathcal{T}^{\text{low}}$  as the final answer; otherwise, we select that from  $\mathcal{T}^{\text{high}}$ .

By introducing this adjustable threshold  $\Delta$ , we enable entities from both the high-score and low-score subtables to be dynamically selected as the answer. This design enhances flexibility and reduces selection bias in the decision process.

**Theoretical Analysis.** In coarse-to-fine optimization, since the final prediction is made based on comparing the highest scores from the high-score and low-score subtables. Thus, the score gap is particularly crucial for mitigating over-smoothing and we theoretically demonstrate how the coarse-to-fine optimization mitigates over-smoothing by amplifying the gap between the highest scores in the two subtables, as shown in Theorem 2.

**Theorem 2 (Lower Bound on Score Gap Between High-score and Low-score Subtables).** *The lower bound on the expected gap between the top scores of the two subtables ( $s_{e_h}$  and  $s_{e_l}$ ) is:*

$$\mathbb{E}[|s_{e_h} - s_{e_l}|] > \left| \left( \frac{1}{N_h^2 + 1} - \frac{1}{(N_l^2 + 1)} \right) \cdot \sigma \right|, \quad (5)$$

where  $N_h$  and  $N_l$  denote the number of entities in high-score and low-score subtables respectively.  $\sigma$  is the standard deviation of the entity score.

We provide a detailed proof of Theorem 2 in Appendix A.2. Based on Theorem 2, we establish the relationship between the score gap and the number of entities. In our setup, the ratio of the number of entities in the low-score subtable to those in the high-score subtable exceeds 1,000. Therefore, based on Theorem 2, we can derive that the lower bound on the expected gap between the top scores of the two subtables is more than  $0.1\sigma$  (Detailed proof of this in Appendix A.2). In comparison, other baseline methods (as shown in Figure 1) exhibit score gaps between correct and incorrect answers are typically less than  $0.02\sigma$ . This demonstrates that our optimization can amplify the score gap, thus mitigating over-smoothing. Building on this, we additionally present Theorem 3 to theoretically demonstrate that coarse-to-fine optimization also improves the quality of KG reasoning.

**Theorem 3 (Effectiveness of Coarse-to-Fine Optimization).** *Let  $P$  and  $P'$  denote the probabilities of correctly identifying the answer with and without coarse-to-fine optimization, respectively. Then, we have  $P > P'$ .*

We provide a detailed proof of Theorem 3 in Appendix A.3.

**Complexity Analysis.** In this paragraph, we compare the complexity of our coarse-to-fine stage with one-stage approach. The time complexities of coarse-to-fine stage and one-stage are  $\mathcal{O}(\max(L_m(|\mathcal{E}|d + |\mathcal{V}|d^2), L_t|\mathcal{V}|d^2) + |\mathcal{V}|\log|\mathcal{V}|)$  and  $\mathcal{O}(\max(L_m(|\mathcal{E}|d + |\mathcal{V}|d^2), L_t|\mathcal{V}|d^2))$ , respectively. We provide detail proof of these in Appendix B.2. Here,  $|\mathcal{V}|$  and  $|\mathcal{E}|$  denote the number of entities and triplets, respectively.  $L_m$  and  $L_t$  represent the number of message passing layers and transformer layers.  $d$  is the dimension of the entity representation. In practice,  $|\mathcal{V}|\log|\mathcal{V}|$  is much smaller than  $|\mathcal{V}|d^2$ . For example, in FB15k-237 dataset [45], the number of entities is 14,541, and the representation dimension is 32. Accordingly,  $|\mathcal{V}|\log|\mathcal{V}|$  is approximately  $10^5$  and  $|\mathcal{V}|d^2$  is approximately  $10^7$ . Therefore, the time complexity of the coarse-to-fine stage remains comparable to that of the one-stage.

## 4 Empirical Evaluation

In this section, we conduct extensive experiments to answer the following research questions: **(RQ1)** Can DuetGraph effectively improve the performance of inductive KG reasoning tasks? **(RQ2)** Can DuetGraph effectively improve the performance of transductive KG reasoning tasks? **(RQ3)** Can DuetGraph demonstrate strong scalability in KG reasoning tasks by achieving high training efficiency? **(RQ4)** How is the effectiveness of the components of DuetGraph? **(RQ5)** Is DuetGraph sensitive to hyperparameter  $k$ , where  $k$  denotes the number of entities in high-score subset?

### 4.1 Experiments setup

**Inductive Datasets.** For inductive reasoning, following Liu et al. [17], we use the same data divisions of FB15k-237 [45], WN18RR [46], and NELL-995 [47]. Each division consists of 4 versions, resulting in 12 subsets in total. Notably, in each subset, the training and test sets contain disjoint sets of entities while sharing the same set of relations.

**Transductive Datasets.** For transductive reasoning, we conduct experiments on four widely utilized KG reasoning datasets: FB15k-237 [45], WN18RR [46], NELL-995 [47], and YAGO3-10 [48], adopting the standard data splits provided by prior works [26, 49].

**Inductive Baselines.** We compare DuetGraph with 8 baseline methods for inductive KG reasoning as shown in Table 1. For completeness, we note that some baselines do not support certain datasets due to limitations in their released code. Details are provided in Appendix C.2.

**Transductive Baselines.** The following four categories of SOTA models are adopted as baselines for comparison with DuetGraph in transductive KG reasoning: *triplet-based models*, *message passing-based models*, *transformer-based models*, *hybrid message passing-transformer models* (including our proposed method and KnowFormer [17]) and other approaches, as shown in Table 2.

**Evaluations Metrics.** The model performance is measured by **Mean Reciprocal Rank (MRR)** [32] and **Hit Rate at  $k$**  (Hits@ $k$ , where  $k \in \{1, 10\}$ ) [32]. Hits@ $k$  assesses whether the true entity of a triplet appears within the top- $k$  ranked candidate entities. If the true entity is ranked  $k$  or



Table 1: Inductive KG reasoning performance for various methods on 12 subsets. (The best results are bolded in red with a yellow highlight. Second-best results are with a blue highlight. Results are either sourced directly from original papers or reproduced based on available code.)

Method	v1			v2			v3			v4		
	MRR	H@1	H@10	MRR	H@1	H@10	MRR	H@1	H@10	MRR	H@1	H@10
<b>FB15k-237</b>												
DRUM [50]	0.333	24.7	47.4	0.395	28.4	59.5	0.402	30.8	57.1	0.410	30.9	59.3
NBFNet [26]	0.442	33.5	57.4	0.514	42.1	68.5	0.476	38.4	63.7	0.453	36.0	62.7
RED-GNN [3]	0.369	30.2	48.3	0.469	38.1	62.9	0.445	35.1	50.3	0.442	34.0	62.1
A*Net [11]	0.457	38.1	58.9	0.510	41.9	67.2	0.476	38.9	62.9	0.466	36.5	64.5
AdaProp [49]	0.310	19.1	55.1	0.471	37.2	65.9	0.471	37.7	63.7	0.454	35.3	63.8
Ingram [51]	0.293	16.7	49.3	0.274	16.3	48.2	0.233	14.0	40.8	0.214	11.4	39.7
KnowFormer [17]	0.466	37.8	60.6	0.532	43.3	70.3	0.494	40.0	65.9	0.480	38.3	65.3
DuetGraph (Ours)	<b>0.507</b>	<b>42.7</b>	<b>63.2</b>	<b>0.549</b>	<b>44.8</b>	<b>72.9</b>	<b>0.518</b>	<b>42.3</b>	<b>69.9</b>	<b>0.501</b>	<b>39.8</b>	<b>69.0</b>
<b>WN18RR</b>												
DRUM [50]	0.666	61.3	77.7	0.646	59.5	74.7	0.380	33.0	47.7	0.627	58.6	70.2
NBFNet [26]	0.741	69.5	<b>82.6</b>	0.704	65.1	79.8	0.452	39.2	56.8	0.641	60.8	69.4
RED-GNN [3]	0.701	65.3	79.9	0.690	63.3	78.0	0.427	36.8	52.4	0.651	60.6	72.1
A*Net [11]	0.727	68.2	81.0	0.704	64.9	80.3	0.441	38.6	54.4	0.661	61.6	74.3
AdaProp [49]	0.733	66.8	80.6	<b>0.715</b>	64.2	<b>82.6</b>	<b>0.474</b>	39.6	<b>58.8</b>	<b>0.662</b>	61.1	<b>75.5</b>
Ingram [51]	0.277	13.0	60.6	0.236	11.2	48.0	0.230	11.6	46.6	0.118	4.1	25.9
SimKGC [52]	0.315	19.2	56.7	0.378	23.9	65.0	0.303	18.6	54.3	0.308	17.5	57.7
KnowFormer [17]	<b>0.752</b>	71.5	81.9	0.709	65.6	81.7	0.467	40.6	57.1	0.646	60.9	72.7
DuetGraph (Ours)	<b>0.758</b>	<b>72.1</b>	81.7	<b>0.719</b>	<b>66.7</b>	81.1	<b>0.501</b>	<b>44.3</b>	<b>62.2</b>	<b>0.662</b>	<b>62.1</b>	73.1
<b>NELL-995</b>												
NBFNet [26]	0.584	50.0	79.5	0.410	27.1	63.5	0.425	26.2	60.6	0.287	25.3	59.1
RED-GNN [3]	0.637	52.2	86.6	0.419	31.9	60.1	0.436	34.5	59.4	0.363	25.9	<b>60.7</b>
AdaProp [49]	0.644	52.2	88.6	0.452	34.4	65.2	0.435	33.7	61.8	0.366	24.7	<b>60.7</b>
Ingram [51]	0.697	57.5	86.5	0.358	25.3	59.6	0.308	19.9	50.9	0.221	12.4	44.0
KnowFormer [17]	<b>0.827</b>	77.0	93.0	0.465	35.7	65.7	0.478	37.8	65.7	0.378	26.7	59.8
DuetGraph (Ours)	<b>0.850</b>	<b>78.5</b>	<b>96.5</b>	<b>0.543</b>	<b>44.4</b>	<b>69.1</b>	<b>0.535</b>	<b>43.2</b>	<b>72.6</b>	<b>0.464</b>	<b>35.4</b>	<b>68.4</b>

higher, the result is recorded as 1; otherwise, it is recorded as 0. Metrics are formalized as follows.

$\text{Hits}@k = \frac{1}{|\mathcal{T}_{\text{test}}|} \sum_{t_i \in \mathcal{T}_{\text{test}}} f(\text{rank}_i)$ , where  $f(x) = \begin{cases} 1, & x \leq k \\ 0, & x > k \end{cases}$  and  $\mathcal{T}_{\text{test}}$  is the test set containing  $|\mathcal{T}_{\text{test}}|$  triplets. Each  $t_i$  is the  $i$ -th test triplet, and  $\text{rank}_i$  represents the position of the correct entity in the ranked list of candidates. MRR is calculated as the average of the reciprocals of the ranks assigned to the correct entities in the prediction results.  $\text{MRR} = \frac{1}{|\mathcal{T}_{\text{test}}|} \sum_{t_i \in \mathcal{T}_{\text{test}}} \left( \frac{1}{\text{rank}_i} \right)$ , where  $\mathcal{T}_{\text{test}}$  is the test set, and  $\text{rank}_i$  represents the rank of the true entity in the candidate list for  $t_i$ .

## 4.2 Performance

To answer (RQ1), we evaluate DuetGraph on 12 datasets. The results, shown in Table 1, demonstrate the strong performance of DuetGraph compared to baseline models. Specifically, DuetGraph surpasses SOTA methods by up to 8.6% improvement in MRR, 8.7% improvement in Hits@1, and 7.7% improvement in Hits@10. It ranks first in Hits@1 on every evaluated version (v1–v4) of the FB15k-237, WN18RR, and NELL-995 datasets, indicating its strong ability to accurately predict the correct entity at the top rank. Importantly, our method relies solely on the structural information of the KG, without relying on external textual features, highlighting its strong generalization capability.

To answer (RQ2), we evaluate the performance of DuetGraph on four widely utilized transductive KG reasoning datasets. Table 2 demonstrates the impressive performance of DuetGraph compared to baseline models. Specifically, DuetGraph demonstrates substantial performance gains over baseline methods, with improvements of up to 37.2% in MRR, 52.8% in Hits@1, and 24.1% in Hits@10.

It is worth noting that in inductive KG reasoning, the entities to be predicted are unseen during training, which not only aligns more closely with real-world scenarios but also poses a greater challenge. Based on these results, DuetGraph exhibits remarkable generalization and adaptability.

Table 2: Transductive KG reasoning performance for various methods on 4 datasets. (The best results are bolded in red with a yellow highlight. Second-best results are with a blue highlight. Results are either sourced directly from original papers or reproduced based on publicly available code. “-” indicates unavailable results due to insufficient information for reproduction. )

Method	FB15k-237			WN18RR			NELL-995			YAGO3-10		
	MRR	H@1	H@10	MRR	H@1	H@10	MRR	H@1	H@10	MRR	H@1	H@10
<b>Triplet-based</b>												
TransE [32]	0.330	23.2	52.6	0.222	1.4	52.8	0.507	42.4	64.8	0.510	41.3	68.1
DistMult [34]	0.358	26.4	55.0	0.455	41.0	54.4	0.531	43.6	60.2	0.531	46.5	60.2
RotatE [35]	0.337	24.1	53.0	0.455	41.0	54.4	0.511	46.5	60.2	0.519	45.3	60.1
HousE [19]	0.361	26.6	55.1	0.511	46.5	60.2	0.519	45.8	61.8	0.571	49.1	71.4
<b>Message passing-based</b>												
CompGCN [12]	0.355	26.4	53.5	0.479	44.3	54.6	0.463	39.2	59.6	0.456	39.2	56.7
NBFNet [26]	0.364	29.4	58.9	0.494	44.4	57.9	0.531	42.4	64.6	0.543	47.7	70.1
RED-GNN [3]	0.374	28.2	58.9	0.519	46.5	60.2	0.521	44.7	64.1	0.556	47.0	70.7
A*Net [11]	0.373	29.4	59.0	0.544	47.1	61.1	0.537	47.7	66.3	0.570	49.1	72.0
AdaProp [49]	0.389	30.2	59.8	0.540	46.8	61.0	0.554	48.5	67.1	0.558	50.2	72.3
ULTRA [53]	0.368	27.2	56.4	0.480	41.4	61.4	0.509	44.1	66.0	0.557	47.1	71.0
<b>Transformer-based</b>												
HittER [54]	0.373	27.9	55.8	0.503	46.2	58.4	0.518	43.7	65.9	0.339	25.1	50.8
KGT5 [55]	0.276	21.0	41.4	0.508	48.7	54.4	-	-	-	0.426	36.8	52.8
N-Former [56]	0.373	27.9	55.6	0.489	44.6	58.1	-	-	-	-	-	-
SAttLE [20]	0.360	26.8	54.5	0.491	45.4	55.8	0.512	42.2	66.0	0.475	36.7	68.2
<b>Others</b>												
MetaSD [29]	0.391	30.0	57.1	0.491	44.7	57.0	0.516	45.5	61.5	OOM	OOM	OOM
RNNLogic [37]	0.354	25.8	54.6	0.469	42.0	56.5	0.463	39.2	59.6	0.466	40.2	58.7
TuckeER-IVR [38]	0.368	27.4	55.5	0.501	46.0	57.9	0.505	42.8	63.7	0.581	50.8	71.2
<b>Hybrid</b>												
KnowFormer [17]	0.430	34.3	60.8	0.579	52.8	68.7	0.566	50.2	67.5	0.615	54.7	73.4
DuetGraph (Ours)	<b>0.456</b>	<b>36.1</b>	<b>62.8</b>	<b>0.594</b>	<b>54.2</b>	<b>70.0</b>	<b>0.593</b>	<b>52.2</b>	<b>71.2</b>	<b>0.632</b>	<b>56.1</b>	<b>74.9</b>

### 4.3 Efficiency

To answer (RQ3), we evaluate Hits@1 throughout training on the FB15k-237 and YAGO3-10, the latter being a large-scale dataset with millions of training triples. We compare DuetGraph with the best models in each category—AdaProp (message passing-based), SAttLE (transformer-based), and KnowFormer (hybrid). As shown in Figure 3, DuetGraph finally achieves SOTA performance on FB15k-237 while reducing training time by nearly 50% compared to the second best method. We also observe from Figure 3 that DuetGraph achieves SOTA performance on YAGO3-10 while requiring less training time compared to other methods. These results show that DuetGraph achieves scalability through high training efficiency. The observed improvement is primarily attributable to this dual-pathway design, which enables parallel training of both local and global pathways.

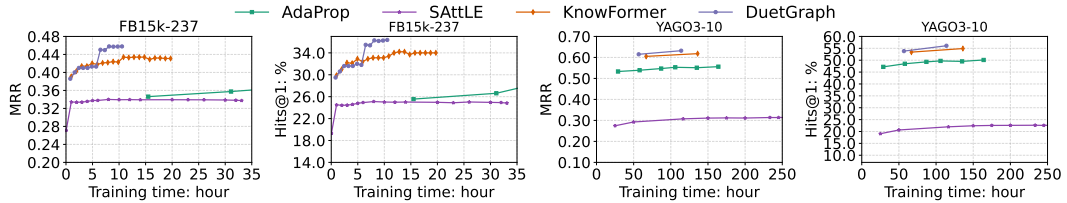


Figure 3: Hits@1 and MRR w.r.t. time on FB15k-237 and YAGO3-10.

### 4.4 Ablation Study

To address (RQ4), we perform an ablation study by removing key components of DuetGraph: (1) the local pathway, (2) the global pathway, (3) the coarse-to-fine reasoning optimization (i.e., reducing DuetGraph model to the dual-pathway fusion alone), (4) the dual-pathway fusion model (i.e., leaving only the coarse-grained reasoning), and (5) the threshold  $\Delta$  in the fine-grained stage, which prevents correction for low-score predictions.



Table 3: Different components ablation study of DuetGraph on 4 transductive KG reasoning datasets. (The best results are bolded in red with a yellow highlight.)

Method	FB15k-237			WN18RR			NELL-995			YAGO3-10		
	MRR	H@1	H@10	MRR	H@1	H@10	MRR	H@1	H@10	MRR	H@1	H@10
<b>DuetGraph</b>	<b>0.456</b>	<b>36.1</b>	<b>62.8</b>	<b>0.594</b>	<b>54.2</b>	<b>70.0</b>	<b>0.593</b>	<b>52.2</b>	<b>71.2</b>	<b>0.632</b>	<b>56.1</b>	<b>74.9</b>
w/o local	0.445	35.1	61.2	0.584	54.1	69.0	0.582	51	70.3	0.617	54.2	73.7
w/o global	0.441	34.9	61.4	0.565	51.7	66.6	0.586	51	69.8	0.614	53.8	74.4
w/o Coarse-to-Fine reasoning	0.429	33.6	61.0	0.571	52.0	67.3	0.555	48.8	67.4	0.612	54.1	73.9
w/o Dual-Pathway fusion model	0.355	25.9	54.7	0.512	46.6	60.6	0.534	46.6	51.2	0.563	48.4	70.7
w/o threshold value $\Delta$	0.395	31.7	55.8	0.551	48.9	66.1	0.544	49.8	66.5	0.595	53.4	70.9

Table 4: Different coarse-grained model ablation study of DuetGraph on 4 transductive KG reasoning datasets. (The best results are bolded in red with a yellow highlight.)

Method	FB15k-237			WN18RR			NELL-995			YAGO3-10		
	MRR	H@1	H@10	MRR	H@1	H@10	MRR	H@1	H@10	MRR	H@1	H@10
KnowFormer [17]	0.430	34.3	60.8	0.579	52.8	68.7	0.566	50.2	67.5	0.615	54.7	73.4
DuetGraph (w/ triplets-based model as coarse model)	<b>0.456</b>	<b>36.1</b>	<b>62.8</b>	<b>0.594</b>	<b>54.2</b>	<b>70.0</b>	<b>0.593</b>	<b>52.2</b>	<b>71.2</b>	<b>0.632</b>	<b>56.1</b>	<b>74.9</b>
DuetGraph (w/ message passing-based model as coarse model)	0.446	35.4	61.3	0.589	53.5	69.0	0.584	51.7	70.2	0.622	55.4	73.9
DuetGraph (w/ transformer-based model as coarse model)	0.445	34.8	62.4	0.586	53.2	69.4	0.579	50.8	70.5	0.624	55.7	74.2

As shown in Table 3, removing either the local or global pathway degrades performance, confirming the necessity of both information types. Eliminating coarse-to-fine reasoning leads to a notable drop in Hits@1, demonstrating its effectiveness in refining predictions. Excluding the dual-pathway module results in the largest performance loss, which underscores its crucial role in reasoning performance. Finally, removing the threshold  $\Delta$  reduces accuracy due to uncorrected errors in cases where the correct entity is excluded from the high-score subset during coarse reasoning.

We additionally evaluate the performance of DuetGraph on four transductive KG reasoning datasets using three different types coarse-grained reasoning models: a triplet-based model (HousE [19]), a message passing-based model (RED-GNN [3]), and a hybrid message passing-transformer model (KnowFormer [17]), which is the SOTA method. As shown in Table 4, DuetGraph, when integrated with any of the three coarse grained models, consistently outperforms its competitors.

#### 4.5 Parameter Analysis

To answer (RQ5), we conduct experiments by varying the hyperparameter  $k$  introduced in Section 3.2 across four different transductive datasets. As shown in Figure 4, DuetGraph is insensitive to the parameter  $k$ , suggesting stable performance. We further conduct hyperparameter experiments on inductive datasets, as presented in Appendix D.2, and obtain consistent results.

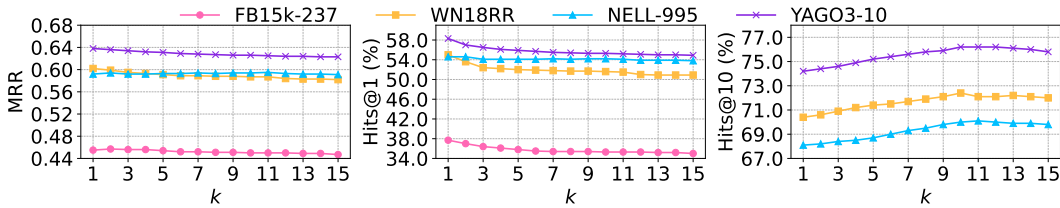


Figure 4: Effect of  $k$  on the performance metrics of KG reasoning for different datasets (Transductive).

## 5 Conclusion

This paper proposes DuetGraph, a coarse-to-fine KG reasoning mechanism with dual-pathway global-local fusion to alleviate score over-smoothing in KG reasoning. DuetGraph mitigates over-smoothing by allocating the processing of local (via message passing) and global (via attention) information to two distinct pathways, rather than stacking them. This design prevents mutual interference and preserves representational discrimination. Experimental results show that DuetGraph outperforms SOTA baselines on both quality and training efficiency.

## References

- [1] Zihao Li, Yuyi Ao, and Jingrui He. Sphere: Expressive and interpretable knowledge graph embedding for set retrieval. In *Proceedings of the 47th International ACM SIGIR Conference on Research and Development in Information Retrieval*, SIGIR '24, page 2629–2634, New York, NY, USA, 2024. Association for Computing Machinery.
- [2] Ying Zhou, Xuanang Chen, Ben He, Zheng Ye, and Le Sun. Re-thinking knowledge graph completion evaluation from an information retrieval perspective. In Enrique Amigó, Pablo Castells, Julio Gonzalo, Ben Carterette, J. Shane Culpepper, and Gabriella Kazai, editors, *SIGIR '22: The 45th International ACM SIGIR Conference on Research and Development in Information Retrieval, Madrid, Spain, July 11 - 15, 2022*, pages 916–926. ACM, 2022.
- [3] Yongqi Zhang and Quanming Yao. Knowledge graph reasoning with relational digraph. In *Proceedings of the ACM web conference 2022*, pages 912–924, 2022.
- [4] Ziqi Yang, Zhaopeng Peng, Zihui Wang, Jianzhong Qi, Chaochao Chen, WeiKe Pan, Chenglu Wen, Cheng Wang, and Xiaoliang Fan. Federated graph learning for cross-domain recommendation. In Amir Globersons, Lester Mackey, Danielle Belgrave, Angela Fan, Ulrich Paquet, Jakub M. Tomczak, and Cheng Zhang, editors, *Advances in Neural Information Processing Systems 38: Annual Conference on Neural Information Processing Systems 2024, NeurIPS 2024, Vancouver, BC, Canada, December 10 - 15, 2024*, 2024.
- [5] Yanpeng Ye, Jie Ren, Shaozhou Wang, Yuwei Wan, Imran Razzak, Bram Hoex, Haofeng Wang, Tong Xie, and Wenjie Zhang. Construction and application of materials knowledge graph in multidisciplinary materials science via large language model. In A. Globerson, L. Mackey, D. Belgrave, A. Fan, U. Paquet, J. Tomczak, and C. Zhang, editors, *Advances in Neural Information Processing Systems*, volume 37, pages 56878–56897. Curran Associates, Inc., 2024.
- [6] Vineeth Venugopal and Elsa Olivetti. Matkg: An autonomously generated knowledge graph in material science. *Scientific Data*, 11(1):217, 2024.
- [7] Yuan Zhang, Xin Sui, Feng Pan, Kaixian Yu, Keqiao Li, Shubo Tian, Arslan Erdengasileng, Qing Han, Wanjiang Wang, Jianan Wang, et al. A comprehensive large-scale biomedical knowledge graph for ai-powered data-driven biomedical research. *Nature Machine Intelligence*, pages 1–13, 2025.
- [8] Zifeng Wang, Zichen Wang, Balasubramaniam Srinivasan, Vassilis N. Ioannidis, Huzefa Rangwala, and Rishita Anubhai. Biobridge: Bridging biomedical foundation models via knowledge graphs. In *The Twelfth International Conference on Learning Representations, ICLR 2024, Vienna, Austria, May 7-11, 2024*. OpenReview.net, 2024.
- [9] Haotong Yang, Zhouchen Lin, and Muhan Zhang. Rethinking knowledge graph evaluation under the open-world assumption. In *Proceedings of the 36th International Conference on Neural Information Processing Systems*, NIPS '22, Red Hook, NY, USA, 2022. Curran Associates Inc.
- [10] Lorenzo Loconte, Nicola Di Mauro, Robert Peharz, and Antonio Vergari. How to turn your knowledge graph embeddings into generative models. In *Proceedings of the 37th International Conference on Neural Information Processing Systems*, NIPS '23, Red Hook, NY, USA, 2023. Curran Associates Inc.
- [11] Zhaocheng Zhu, Xinyu Yuan, Michael Galkin, Louis-Pascal Xhonneux, Ming Zhang, Maxime Gazeau, and Jian Tang. A\* net: A scalable path-based reasoning approach for knowledge graphs. *Advances in Neural Information Processing Systems*, 36, 2024.
- [12] Shikhar Vashishth, Soumya Sanyal, Vikram Nitin, and Partha Talukdar. Composition-based multi-relational graph convolutional networks. *arXiv preprint arXiv:1911.03082*, 2019.
- [13] Thomas N. Kipf and Max Welling. Semi-supervised classification with graph convolutional networks. In *International Conference on Learning Representations*, 2017.
- [14] Zhanghao Wu, Paras Jain, Matthew A. Wright, Azalia Mirhoseini, Joseph E. Gonzalez, and Ion Stoica. Representing long-range context for graph neural networks with global attention. In *Proceedings of the 35th International Conference on Neural Information Processing Systems*, NIPS '21, Red Hook, NY, USA, 2021. Curran Associates Inc.

- [15] Qitian Wu, Wentao Zhao, Zenan Li, David Wipf, and Junchi Yan. Nodeformer: a scalable graph structure learning transformer for node classification. In *Proceedings of the 36th International Conference on Neural Information Processing Systems, NIPS '22*, Red Hook, NY, USA, 2022. Curran Associates Inc.
- [16] Van Thuy Hoang and O-Joun Lee. Transitivity-preserving graph representation learning for bridging local connectivity and role-based similarity. In *Proceedings of the Thirty-Eighth AAAI Conference on Artificial Intelligence and Thirty-Sixth Conference on Innovative Applications of Artificial Intelligence and Fourteenth Symposium on Educational Advances in Artificial Intelligence, AAAI'24/IAAI'24/EAAI'24*. AAAI Press, 2024.
- [17] Junnan Liu, Qianren Mao, Weifeng Jiang, and Jianxin Li. Knowformer: revisiting transformers for knowledge graph reasoning. *arXiv preprint arXiv:2409.12865*, 2024.
- [18] Fobo Shi, Duantengchuan Li, Xiaoguang Wang, Bing Li, and Xindong Wu. Tgformer: A graph transformer framework for knowledge graph embedding. *IEEE Transactions on Knowledge and Data Engineering*, 2024.
- [19] Rui Li, Jianan Zhao, Chaozhuo Li, Di He, Yiqi Wang, Yuming Liu, Hao Sun, Senzhang Wang, Weiwei Deng, Yanming Shen, et al. House: Knowledge graph embedding with householder parameterization. In *International conference on machine learning*, pages 13209–13224. PMLR, 2022.
- [20] Peyman Baghershashi, Reshad Hosseini, and Hadi Moradi. Self-attention presents low-dimensional knowledge graph embeddings for link prediction. *Knowledge-Based Systems*, 260:110124, 2023.
- [21] Guangtao Wang, Rex Ying, Jing Huang, and Jure Leskovec. Improving graph attention networks with large margin-based constraints. *CoRR*, abs/1910.11945, 2019.
- [22] Qimai Li, Zhichao Han, and Xiao-Ming Wu. Deeper insights into graph convolutional networks for semi-supervised learning. In *Proceedings of the AAAI conference on artificial intelligence*, volume 32, 2018.
- [23] Arvind Neelakantan, Benjamin Roth, and Andrew McCallum. Compositional vector space models for knowledge base completion. In *Proceedings of the 53rd Annual Meeting of the Association for Computational Linguistics and the 7th International Joint Conference on Natural Language Processing of the Asian Federation of Natural Language Processing, ACL 2015, July 26-31, 2015, Beijing, China, Volume 1: Long Papers*, pages 156–166. The Association for Computer Linguistics, 2015.
- [24] Deli Chen, Yankai Lin, Wei Li, Peng Li, Jie Zhou, and Xu Sun. Measuring and relieving the over-smoothing problem for graph neural networks from the topological view. In *Proceedings of the AAAI conference on artificial intelligence*, volume 34, pages 3438–3445, 2020.
- [25] Hongwei Wang, Hongyu Ren, and Jure Leskovec. Relational message passing for knowledge graph completion. In *Proceedings of the 27th ACM SIGKDD Conference on Knowledge Discovery & Data Mining, KDD '21*, page 1697–1707, New York, NY, USA, 2021. Association for Computing Machinery.
- [26] Zhaocheng Zhu, Zuobai Zhang, Louis-Pascal Xhonneux, and Jian Tang. Neural bellman-ford networks: A general graph neural network framework for link prediction. *Advances in Neural Information Processing Systems*, 34:29476–29490, 2021.
- [27] Luca Franceschi, Mathias Niepert, Massimiliano Pontil, and Xiao He. Learning discrete structures for graph neural networks. In *International conference on machine learning*, pages 1972–1982. PMLR, 2019.
- [28] Uri Alon and Eran Yahav. On the bottleneck of graph neural networks and its practical implications. In *International Conference on Learning Representations*.
- [29] Yunshui Li, Junhao Liu, Chengming Li, and Min Yang. Self-distillation with meta learning for knowledge graph completion. *arXiv preprint arXiv:2305.12209*, 2023.
- [30] Zezhong Xu, Peng Ye, Hui Chen, Meng Zhao, Huajun Chen, and Wen Zhang. Ruleformer: Context-aware rule mining over knowledge graph. In Nicoletta Calzolari, Chu-Ren Huang, Hansaem Kim, James Pustejovsky, Leo Wanner, Key-Sun Choi, Pum-Mo Ryu, Hsin-Hsi Chen, Lucia Donatelli, Heng Ji, Sadao Kurohashi, Patrizia Paggio, Nianwen Xue, Seokhwan Kim, Younggyun Hahn, Zhong He, Tony Kyungil Lee, Enrico Santus, Francis Bond, and Seung-Hoon

- Na, editors, *Proceedings of the 29th International Conference on Computational Linguistics*, pages 2551–2560, Gyeongju, Republic of Korea, October 2022. International Committee on Computational Linguistics.
- [31] Linfeng Song, Ante Wang, Jinsong Su, Yue Zhang, Kun Xu, Yubin Ge, and Dong Yu. Structural information preserving for graph-to-text generation. In Dan Jurafsky, Joyce Chai, Natalie Schluter, and Joel R. Tetreault, editors, *Proceedings of the 58th Annual Meeting of the Association for Computational Linguistics, ACL 2020, Online, July 5-10, 2020*, pages 7987–7998. Association for Computational Linguistics, 2020.
  - [32] Antoine Bordes, Nicolas Usunier, Alberto Garcia-Duran, Jason Weston, and Oksana Yakhnenko. Translating embeddings for modeling multi-relational data. *Advances in neural information processing systems*, 26, 2013.
  - [33] Théo Trouillon, Johannes Welbl, Sebastian Riedel, Éric Gaussier, and Guillaume Bouchard. Complex embeddings for simple link prediction. In *International conference on machine learning*, pages 2071–2080. PMLR, 2016.
  - [34] Bishan Yang, Wen-tau Yih, Xiaodong He, Jianfeng Gao, and Li Deng. Embedding entities and relations for learning and inference in knowledge bases. *arXiv preprint arXiv:1412.6575*, 2014.
  - [35] Zhiqing Sun, Zhi-Hong Deng, Jian-Yun Nie, and Jian Tang. Rotate: Knowledge graph embedding by relational rotation in complex space. *arXiv preprint arXiv:1902.10197*, 2019.
  - [36] Yunshui Li, Junhao Liu, Min Yang, and Chengming Li. Self-distillation with meta learning for knowledge graph completion. In Yoav Goldberg, Zornitsa Kozareva, and Yue Zhang, editors, *Findings of the Association for Computational Linguistics: EMNLP 2022*, pages 2048–2054, Abu Dhabi, United Arab Emirates, December 2022. Association for Computational Linguistics.
  - [37] Meng Qu, Junkun Chen, Louis-Pascal Xhonneux, Yoshua Bengio, and Jian Tang. Rnnlogic: Learning logic rules for reasoning on knowledge graphs. In *International Conference on Learning Representations*.
  - [38] Changyi Xiao and Yixin Cao. Knowledge graph completion by intermediate variables regularization. *Advances in Neural Information Processing Systems*, 37:110218–110245, 2024.
  - [39] Tomás Mikolov, Ilya Sutskever, Kai Chen, Gregory S. Corrado, and Jeffrey Dean. Distributed representations of words and phrases and their compositionality. In Christopher J. C. Burges, Léon Bottou, Zoubin Ghahramani, and Kilian Q. Weinberger, editors, *Advances in Neural Information Processing Systems 26: 27th Annual Conference on Neural Information Processing Systems 2013. Proceedings of a meeting held December 5-8, 2013, Lake Tahoe, Nevada, United States*, pages 3111–3119, 2013.
  - [40] Diederik P Kingma and Jimmy Ba. Adam: A method for stochastic optimization. *arXiv preprint arXiv:1412.6980*, 2014.
  - [41] Qitian Wu, Wentao Zhao, Chenxiao Yang, Hengrui Zhang, Fan Nie, Haitian Jiang, Yatao Bian, and Junchi Yan. Sgformer: Simplifying and empowering transformers for large-graph representations, 2024.
  - [42] Shuo Yin and Guoqiang Zhong. Lgi-gt: graph transformers with local and global operators interleaving. In *Proceedings of the Thirty-Second International Joint Conference on Artificial Intelligence, IJCAI '23*, 2023.
  - [43] Takeru Miyato, Toshiki Kataoka, Masanori Koyama, and Yuichi Yoshida. Spectral normalization for generative adversarial networks. In *6th International Conference on Learning Representations, ICLR 2018, Vancouver, BC, Canada, April 30 - May 3, 2018, Conference Track Proceedings*. OpenReview.net, 2018.
  - [44] Aladin Virmaux and Kevin Scaman. Lipschitz regularity of deep neural networks: analysis and efficient estimation. In Samy Bengio, Hanna M. Wallach, Hugo Larochelle, Kristen Grauman, Nicolò Cesa-Bianchi, and Roman Garnett, editors, *Advances in Neural Information Processing Systems 31: Annual Conference on Neural Information Processing Systems 2018, NeurIPS 2018, December 3-8, 2018, Montréal, Canada*, pages 3839–3848, 2018.
  - [45] Kristina Toutanova and Danqi Chen. Observed versus latent features for knowledge base and text inference. In *Proceedings of the 3rd workshop on continuous vector space models and their compositionality*, pages 57–66, 2015.

- [46] Tim Dettmers, Pasquale Minervini, Pontus Stenetorp, and Sebastian Riedel. Convolutional 2d knowledge graph embeddings. In *Proceedings of the AAAI conference on artificial intelligence*, volume 32, 2018.
- [47] Wenhan Xiong, Thien Hoang, and William Yang Wang. Deeppath: A reinforcement learning method for knowledge graph reasoning. *arXiv preprint arXiv:1707.06690*, 2017.
- [48] Farzaneh Mahdisoltani, Joanna Biega, and Fabian M Suchanek. Yago3: A knowledge base from multilingual wikipedias. In *CIDR*, 2013.
- [49] Yongqi Zhang, Zhanke Zhou, Quanming Yao, Xiaowen Chu, and Bo Han. Adaprop: Learning adaptive propagation for graph neural network based knowledge graph reasoning. In *Proceedings of the 29th ACM SIGKDD Conference on Knowledge Discovery and Data Mining*, pages 3446–3457, 2023.
- [50] Ali Sadeghian, Mohammadreza Armandpour, Patrick Ding, and Daisy Zhe Wang. *DRUM: end-to-end differentiable rule mining on knowledge graphs*. Curran Associates Inc., Red Hook, NY, USA, 2019.
- [51] Jaejun Lee, Chanyoung Chung, and Joyce Jiyoung Whang. Ingram: inductive knowledge graph embedding via relation graphs. In *Proceedings of the 40th International Conference on Machine Learning, ICML’23*. JMLR.org, 2023.
- [52] Liang Wang, Wei Zhao, Zhuoyu Wei, and Jingming Liu. Simkgc: Simple contrastive knowledge graph completion with pre-trained language models. *arXiv preprint arXiv:2203.02167*, 2022.
- [53] Mikhail Galkin, Xinyu Yuan, Hesham Mostafa, Jian Tang, and Zhaocheng Zhu. Towards foundation models for knowledge graph reasoning. *arXiv preprint arXiv:2310.04562*, 2023.
- [54] Sanxing Chen, Xiaodong Liu, Jianfeng Gao, Jian Jiao, Ruofei Zhang, and Yangfeng Ji. Hitter: Hierarchical transformers for knowledge graph embeddings. *arXiv preprint arXiv:2008.12813*, 2020.
- [55] Apoorv Saxena, Adrian Kochsiek, and Rainer Gemulla. Sequence-to-sequence knowledge graph completion and question answering. *arXiv preprint arXiv:2203.10321*, 2022.
- [56] Yang Liu, Zequn Sun, Guangyao Li, and Wei Hu. I know what you do not know: Knowledge graph embedding via co-distillation learning. In *Proceedings of the 31st ACM International Conference on Information & Knowledge Management, CIKM ’22*, page 1329–1338, New York, NY, USA, 2022. Association for Computing Machinery.
- [57] Qingyang Li, Yanru Zhong, and Yuchu Qin. Mocokgc: Momentum contrast entity encoding for knowledge graph completion. In *Proceedings of the 2024 Conference on Empirical Methods in Natural Language Processing*, pages 14940–14952, 2024.
- [58] Weijia Shi, Anirudh Ajith, Mengzhou Xia, Yangsibo Huang, Daogao Liu, Terra Blevins, Danqi Chen, and Luke Zettlemoyer. Detecting pretraining data from large language models. In *The Twelfth International Conference on Learning Representations, ICLR 2024, Vienna, Austria, May 7-11, 2024*. OpenReview.net, 2024.
- [59] Antoine Bordes, Nicolas Usunier, Alberto Garcia-Duran, Jason Weston, and Oksana Yakhnenko. Translating embeddings for modeling multi-relational data. In C.J. Burges, L. Bottou, M. Welling, Z. Ghahramani, and K.Q. Weinberger, editors, *Advances in Neural Information Processing Systems*, volume 26. Curran Associates, Inc., 2013.
- [60] Tim Dettmers, Pasquale Minervini, Pontus Stenetorp, and Sebastian Riedel. Convolutional 2d knowledge graph embeddings. In *Proceedings of the Thirty-Second AAAI Conference on Artificial Intelligence and Thirtieth Innovative Applications of Artificial Intelligence Conference and Eighth AAAI Symposium on Educational Advances in Artificial Intelligence, AAAI’18/IAAI’18/EAAI’18*. AAAI Press, 2018.
- [61] Wenhan Xiong, Thien Hoang, and William Yang Wang. DeepPath: A reinforcement learning method for knowledge graph reasoning. In Martha Palmer, Rebecca Hwa, and Sebastian Riedel, editors, *Proceedings of the 2017 Conference on Empirical Methods in Natural Language Processing*, pages 564–573, Copenhagen, Denmark, September 2017. Association for Computational Linguistics.
- [62] Thomas Rebele, Fabian Suchanek, Johannes Hoffart, Joanna Biega, Erdal Kuzey, and Gerhard Weikum. Yago: A multilingual knowledge base from wikipedia, wordnet, and geonames. In *The Semantic Web – ISWC 2016: 15th International Semantic Web Conference, Kobe,*

*Japan, October 17–21, 2016, Proceedings, Part II*, page 177–185, Berlin, Heidelberg, 2016. Springer-Verlag.

- [63] Kexin Huang, Payal Chandak, Qianwen Wang, Shreyas Havaladar, Akhil Vaid, Jure Leskovec, Girish N Nadkarni, Benjamin S Glicksberg, Nils Gehlenborg, and Marinka Zitnik. A foundation model for clinician-centered drug repurposing. *Nature Medicine*, 30(12):3601–3613, 2024.



## Contents of Appendix

---

<b>A</b>	<b>Proofs of theorems</b>	<b>16</b>
A.1	Dual-Pathway Global-Local Fusion Model Effectively Alleviating Over-Smoothing.	16
A.2	Coares-to-Fine Reasoning Optimization Alleviates the over-smoothing in KG. . . .	17
A.3	Coarse-to-Fine Reasoning Optimization Improves the Quality of KG Reasoning. .	18
<b>B</b>	<b>Time complexity computation</b>	<b>18</b>
B.1	Time Complexity Computation of Dual-Pathway Global-Local Fusion Model. . . .	18
B.2	Time Complexity Computation of Coarse-to-Fine Stage. . . . .	18
<b>C</b>	<b>Additional baseline discussion</b>	<b>19</b>
C.1	DuetGraph v.s. Methods based on pre-trained language models. . . . .	19
C.2	Baseline details. . . . .	20
<b>D</b>	<b>Experimental Details</b>	<b>20</b>
D.1	Dataset Statistics . . . . .	20
D.2	Hyperparameters Setup . . . . .	21
D.3	Random Initialization. . . . .	21
<b>E</b>	<b>Limitations and Broader Impacts</b>	<b>22</b>
E.1	Limitations . . . . .	22
E.2	Broader Impacts . . . . .	22

---

## A Proofs of theorems

In this section, we provide the theorem proofs of in method part, including 1) why our proposed dual-pathway global-local fusion model can alleviate the over-smoothing in KG; 2) why our proposed coarse-to-fine reasoning optimization can alleviate the over-smoothing in KG; 3) why our proposed coarse-to-fine reasoning optimization can improve the quality of KG reasoning.

### A.1 Dual-Pathway Global-Local Fusion Model Effectively Alleviating Over-Smoothing.

*Proof.* Let entity initial representation is denoted as  $X^{(0)} \in \mathbb{R}^{n \times d}$ , symmetrically normalized adjacency matrix in message passing networks is denoted as  $A \in \mathbb{R}^{n \times n}$ . The attention matrix computed by a single layer of global attention is denoted as  $P \in \mathbb{R}^{n \times n}$ . We construct a weight matrix of one-pathway model stacked with  $L$  message passing layers and a transformer layer defined as:

$$\mathcal{M}_O = PA^L \quad (6)$$

We construct a weight matrix of dual-pathway fusion model defined as:

$$\mathcal{M}_D = \alpha A^L + (1 - \alpha)P \quad (7)$$

where  $\alpha$  is the learnable parameter in Equation 1. We first focus on the entity representation obtained after  $\ell$  iterations:

$$X^{(\ell)} = \mathcal{M}^\ell X^{(0)}, \mathcal{M} \in \{\mathcal{M}_O, \mathcal{M}_D\} \quad (8)$$

According to basic properties of the matrix paradigm, we can get spectral norm of  $X^{(m)}$  satisfies

$$\|X^{(\ell)}\|_2 = \|\mathcal{M}^\ell X^{(0)}\|_F \leq \|\mathcal{M}^\ell\|_2 \|X^{(0)}\|_2 \leq (\sigma_{\max}(\mathcal{M}))^\ell \|X^{(0)}\|_2 \quad (9)$$

The representation discrepancy between any two entities  $u$  and  $v$  satisfies

$$\|x_u^{(\ell)} - x_v^{(\ell)}\|_2 \leq \|x_u^{(\ell)}\|_2 + \|x_v^{(\ell)}\|_2 \leq 2\|X^{(\ell)}\|_2 \leq 2(\sigma_{\max}(\mathcal{M}))^\ell \|X^{(0)}\|_2 \quad (10)$$

Then, entity representations are mapped to scalar scores through a multilayer perceptron (MLP). According to the principle of Lipschitz continuity, the score gap between any two entities can be bounded by

$$|S_u - S_v| \leq L_f \cdot \|x_u^{(\ell)} - x_v^{(\ell)}\|_2 \leq 2L_f(\sigma_{\max}(\mathcal{M}))^\ell \|X^{(0)}\|_2 \quad (11)$$

where  $f: \mathbb{R}^d \rightarrow \mathbb{R}$  denotes the MLP and  $L_f$  is the Lipschitz constant [44]. Since  $A$  is a symmetrically normalized adjacency matrix, spectral theory ensures that its eigenvalues  $\{\lambda_i\}_{i=1}^n$  satisfy  $1 = \lambda_1 > \lambda_2 \geq \dots \geq \lambda_n > -1$ . Hence, we conclude that largest eigenvalue of  $A^L$  is equal to 1, and its largest singular value  $\sigma_{\max}(A^L)$  is equal to 1.

Since the attention matrix  $P$  is row-stochastic, its largest eigenvalue is 1, and all other eigenvalues satisfy  $|\mu_i| < 1$ . According to the definition of singular values, it follows that the largest singular value  $\sigma_{\max}(P)$  of  $P$  is less than 1.

Therefore, we can get

$$\sigma_{\max}(\mathcal{M}_O) = \sigma_{\max}(PA^L) \leq \sigma_{\max}(P) \cdot \sigma_{\max}(A^L) = \sigma_{\max}(P) < 1 \quad (12)$$

and since the spectral norm and the maximum singular value are equal we can get

$$\sigma_{\max}(\mathcal{M}_D) = \|\alpha A^L + (1 - \alpha)P\|_2 \leq \|\alpha A^L\|_2 + \|(1 - \alpha)P\|_2 \leq \alpha \|A^L\|_2 + (1 - \alpha)\|P\|_2 < 1 \quad (13)$$

Then, we have

$$\sigma_{\max}(\mathcal{M}) < 1, \quad \mathcal{M} \in \{\mathcal{M}_O, \mathcal{M}_D\} \quad (14)$$

Since the spectral norm and the maximum singular value are equal, we can use the inverse triangle inequality to derive the following:

$$\sigma_{\max}(\mathcal{M}_D) = \|\alpha A^L + (1 - \alpha)P\|_2 \geq \|\alpha A^L\|_2 - \|(1 - \alpha)P\|_2 = |\alpha \cdot 1 - (1 - \alpha)\sigma_{\max}(P)| \quad (15)$$

According to Equation 12, we have

$$\sigma_{\max}(\mathcal{M}_D) \geq \alpha - (1 - \alpha)\sigma_{\max}(P) \geq \alpha - (1 - \alpha)\sigma_{\max}(\mathcal{M}_O) \quad (16)$$

Therefore, as long as the learnable parameter  $\alpha$  is less than  $\frac{\sigma_{\max}(\mathcal{M}_D) + \sigma_{\max}(\mathcal{M}_O)}{1 + \sigma_{\max}(\mathcal{M}_O)}$ ,  $\sigma_{\max}(\mathcal{M}_D)$  will necessarily be greater than  $\sigma_{\max}(\mathcal{M}_O)$ . The result of Equation 11 indicates that as the number of iteration  $\ell$  increases, the score gap between any two entities will decrease exponentially with respect  $\sigma_{\max}(\mathcal{M})$ . This implies that If  $\alpha < \frac{\sigma_{\max}(\mathcal{M}_D) + \sigma_{\max}(\mathcal{M}_O)}{1 + \sigma_{\max}(\mathcal{M}_O)}$ , the score gap upper bound of the the dual-pathway model is greater than that of the one-pathway model and the dual-pathway model shows a slower decrease of the score gap upper bound. Consequently, dual-pathway model effectively mitigates the oversmoothing.  $\square$

## A.2 Coares-to-Fine Reasoning Optimization Alleviates the over-smoothing in KG.

*Proof.* For a set of scores  $\{s_1, s_2, \dots, s_k\}$ , set a score threshold  $t = \mu' + \frac{\sigma'}{k}$ , where  $\mu'$  is the mean of this set of scores and  $\sigma'$  is the standard deviation of this set of scores. Using Cantelli inequality,

$$P(s_i \geq t) = P(s_i \geq \mu' + \frac{\sigma'}{k}) \geq \frac{(\frac{\sigma'}{k})^2}{\sigma'^2 + (\frac{\sigma'}{k})^2} = \frac{1}{k^2 + 1} \quad (17)$$

The probability that at least one  $s_i$  of the  $k$  scores is more than  $t$  is

$$P(\max_i s_i \geq t) \geq 1 - \left(1 - \frac{1}{k^2 + 1}\right)^k \approx \frac{k}{k^2 + 1} \quad (18)$$

Therefore,

$$\mathbb{E}[\max_i s_i] \geq t \cdot P(\max_i s_i \geq t) \geq (\mu' + \frac{\sigma'}{k}) \cdot P(\max_i s_i \geq t) = (\mu' + \frac{\sigma'}{k}) \cdot \frac{k}{k^2 + 1} \quad (19)$$

Let the scores of candidate entities in fine-stage follow a distribution with mean  $\mu$  and standard deviation  $\sigma$ . Let the total number of entities be  $N$ , with the high-score subset containing  $N_h$  entities and low-confidence subset containing  $N_l$  entities. Denote the maximum score within the high-score subset as

$$S_{e_h} = \max_{i=1, \dots, N_h} s_i \quad (20)$$

Denote the maximum score within the low-score subset as

$$S_{e_l} = \max_{i=N_h+1, \dots, N} s_i \quad (21)$$

According to Eqn 19, then the expectation of the maximum of the two subsets satisfies

$$\begin{aligned} \mathbb{E}[S_{e_h}] &\geq (\mu + \frac{\sigma}{N_h}) \cdot \frac{N_h}{N_h^2 + 1} \\ \mathbb{E}[S_{e_l}] &\geq (\mu + \frac{\sigma}{N_l}) \cdot \frac{N_l}{N_l^2 + 1} \end{aligned} \quad (22)$$

The gap between the two is

$$\begin{aligned} |\mathbb{E}[S_{e_h}] - \mathbb{E}[S_{e_l}]| &\geq \left| (\mu + \frac{\sigma}{N_h}) \cdot \frac{N_h}{N_h^2 + 1} - (\mu + \frac{\sigma}{N_l}) \cdot \frac{N_l}{N_l^2 + 1} \right| \\ &= \left| \left( \frac{N_h}{N_h^2 + 1} - \frac{N_l}{N_l^2 + 1} \right) \cdot \mu - \left( \frac{1}{N_h^2 + 1} - \frac{1}{N_l^2 + 1} \right) \cdot \sigma \right| \end{aligned} \quad (23)$$

In our implementation,  $N_h$  is less than 10 and the number of entity in all datasets is more than 10000. Then, we have  $\frac{N_l}{N_h} > 1000$ , and the function  $f(x) = \frac{x}{x^2+1}$  is monotonically decreasing for  $x > 1$ . Therefore,

$$\begin{aligned} |\mathbb{E}[S_{e_h}] - \mathbb{E}[S_{e_l}]| &\geq \left| \left( \frac{1}{N_h^2 + 1} - \frac{1}{N_l^2 + 1} \right) \cdot \sigma \right| \\ &\geq \left| \left( \frac{1}{N_h^2 + 1} - \frac{1}{(1000N_h)^2 + 1} \right) \cdot \sigma \right| \\ &\approx \frac{1}{N_h^2 + 1} \cdot \sigma > 0.1 \cdot \sigma \end{aligned} \quad (24)$$

By Jensen's inequality, we have

$$\mathbb{E}[|S_{e_h} - S_{e_l}|] > |\mathbb{E}[S_{e_h}] - \mathbb{E}[S_{e_l}]| > 0.1 \cdot \sigma \quad (25)$$

We have demonstrate that, in our coarse-to-fine reasoning optimization, the expected score gap between the high-score and low-score subsets is at least 0.1 times the standard deviation. In comparison, other baseline methods (as shown in Figure 1) exhibit score gaps between correct and incorrect answers are typically less than  $0.02\sigma$ . This demonstrates that our optimization can amplifying the score gap, thus mitigating over-smoothing.

□

### A.3 Coarse-to-Fine Reasoning Optimization Improves the Quality of KG Reasoning.

*Proof.* In coarse-grained reasoning, the candidate entities are divided into two subsets, the high-score subset is denoted as  $\mathcal{T}^{high}$ . The highest-scoring entity in each subset, as computed by our proposed dual-pathway fusion model, is denoted as:

$$e_h = \arg \max_{e \in \mathcal{T}^{high}} s(e), \quad e_l = \arg \max_{e \notin \mathcal{T}^{high}} s(e). \quad (26)$$

where the  $s(\cdot)$  denotes score computing by dual-pathway fusion model. Let  $P_\Delta$  denote the probability that the difference between  $e_h$  and  $e_l$  is less than or equal to  $\Delta$ , i.e.  $P_\Delta = P(e_l - e_h \leq \Delta)$

Let  $P$  and  $P'$  denotes the probabilities of correctly identifying the answer with and without coarse-to-fine optimization, respectively. Let event  $A$  denote that the HousE model assigns the ground-truth answer a score that ranks within the top- $k$  among all candidate entities, and event  $B$  denote that our proposed dual-pathway model correctly infers the ground-truth answer. Therefore, the probability that coarse-to-fine reasoning accurately infers the correct answer is:

$$\begin{aligned} P &= P_\Delta \cdot P(B | A) + (1 - P_\Delta) \cdot P' \\ &= P_\Delta \cdot P(B | A) + P' - P_\Delta \cdot P' \\ &= (P(B | A) - P') \cdot P_\Delta + P' \end{aligned} \quad (27)$$

In the following, we compare the magnitude relationship between  $P(B | A)$  and  $P'$ .  $P(B | A)$  represents the probability of event  $B$  occurring given that event  $A$  has occurred. Specifically, the probability that the dual-pathway fusion model correctly infers the correct answer given that the correct answer is ranked within the high-score subset by coarse-grained reasoning. Evidently, the probability of the dual-pathway fusion model correctly inferring the correct answer is higher when the correct answer is already ranked within the high-score subset by coarse stage, compared to the unconditional probability of the dual-pathway fusion model's correct inference. This is because the high-score subset from coarse provides the dual-pathway fusion model with a more focused and promising subset.

Therefore, we can obtain that  $P(B | A) \geq P'$  which leads to  $P \geq P'$ , thus demonstrating that the probability that coarse-to-fine reasoning optimization accurately infers the correct answer is more than the probability that dual-pathway fusion model without coarse-to-fine optimization correctly infers the correct answer.  $\square$

## B Time complexity computation

In this section, we provide details of time complexity computation in Section 3.1 and Section 3.2

### B.1 Time Complexity Computation of Dual-Pathway Global-Local Fusion Model.

**Time complexity of dual-pathway fusion model.** We assume dual-pathway fusion model includes  $L_m$  message passing layers and  $L_t$  transformer layers. Here,  $|\mathcal{V}|$  and  $|\mathcal{E}|$  respectively denote the number of entities and triplets and  $d$  is the dimension of entity representation. For each message passing layer, its time complexity is  $\mathcal{O}(|\mathcal{E}|d + |\mathcal{V}|d^2)$ . For each transformer layer, its time complexity is  $\mathcal{O}(|\mathcal{V}|d^2)$ . Because of message passing layer and transformer in parallel, the overall time complexity of our dual-pathway fusion model is  $\mathcal{O}(\max(L_m(|\mathcal{E}|d + |\mathcal{V}|d^2), L_t|\mathcal{V}|d^2))$ .

**Time complexity of one-pathway model.** We assume one-pathway fusion model includes  $L_m$  message passing layers and  $L_t$  transformer layers. For each message passing layer, its time complexity is  $\mathcal{O}(|\mathcal{E}|d + |\mathcal{V}|d^2)$ . Here,  $|\mathcal{V}|$  and  $|\mathcal{E}|$  respectively denote the number of entities and triplets and  $d$  is the dimension of entity representation. For each transformer layer, its time complexity is  $\mathcal{O}(|\mathcal{V}|d^2)$ . Because message passing layer and transformer is sequential, the overall time complexity of our dual-pathway fusion model are  $\mathcal{O}(L_m|\mathcal{E}|d + (L_m + L_t)|\mathcal{V}|d^2)$ .

### B.2 Time Complexity Computation of Coarse-to-Fine Stage.

The coarse-to-fine reasoning stage has two additional operations of coarse-grained reasoning and sorting all entities compared to one-stage. In coarse-to-fine reasoning, parallel reasoning with coarse

Table 5: Transductive KG reasoning performance for DuetGraph, SimKGC and MoCoKGC on FB15k-237 and WN18RR. (The best results are bolded in red with a yellow highlight. )

Value	FB15k-237			WN18RR		
	MRR	H@1	H@10	MRR	H@1	H@10
SimKGC	0.336	24.9	51.1	0.666	58.5	<b>80.0</b>
MoCoKGC	0.391	29.6	43.1	<b>0.742</b>	<b>66.5</b>	79.2
DuetGraph(ours)	<b>0.456</b>	<b>36.1</b>	<b>62.8</b>	0.594	54.2	70.0

model and fine model. Moreover, the time complexity of the coarse model we employ is  $\mathcal{O}(|\mathcal{E}|d)$  where  $|\mathcal{E}|$  denote the number of triplets and  $d$  is the dimension of entity representation. The time complexity of this sorting process is  $\mathcal{O}(|\mathcal{V}|\log|\mathcal{V}|)$ , where  $|\mathcal{V}|$  denote the number of entities. The one-stage reasoning only includes dual-pathway fusion model. Therefore, the overall time complexity of the coarse-to-fine reasoning stage is  $\mathcal{O}(\max(L_m(|\mathcal{E}|d + |\mathcal{V}|d^2), L_t|\mathcal{V}|d^2) + |\mathcal{V}|\log|\mathcal{V}|)$ .

## C Additional baseline discussion

### C.1 DuetGraph v.s. Methods based on pre-trained language models.

We observe that language model-based reasoning methods such as SimKGC [52] and MoCoKGC [57] achieve unusually high results on WN18RR, but perform poorly on other datasets, as shown in Table 5. To better understand this phenomenon, we take these two methods as representative examples for further analysis. We note that WN18RR is derived from WordNet, a large lexical database of English that naturally encodes rich semantic relations between words. Pretrained language models are well-suited to capturing such general semantic information, which may explain their strong performance on WN18RR. In contrast, FB15k-237 involves more domain-specific relational knowledge, which poses greater challenges for these models, leading to weaker performance(as shown in Table 5).

Additionally, we consider the possibility that the textual descriptions of entities in WN18RR may have appeared in the pretraining corpus of language models, potentially leading to data leakage. Therefore, we adopt the detection method proposed by [58] to estimate the proportion of WN18RR entity texts that are likely included in the pretraining data of the language model used by SimKGC and MoCoKGC (i.e., bert-base-uncased).

Specifically, for an entity text, select the  $\epsilon$  of tokens with the lowest predicted probabilities from the language model. Then, compute the average log-likelihood of these low-probability tokens. If the average log-likelihood exceeds a certain threshold, we consider that the text is likely to have appeared in the language model’s pre-training data.

The detailed results are presented in Table 6. We observe that even under smaller  $\epsilon$  (e.g.,10% and 20%) that means selecting the  $\epsilon$  of tokens that are most difficult to be recognized by the language model, over 70% of the entity texts in WN18RR appear to be memorized by the language model, suggesting a significant potential for data leakage.

Table 6: Pre-training overlap rate under varying  $\epsilon$ , where  $\epsilon$  represents the proportion of low probability tokens predicted by language model.

$\epsilon$	Pretraining Overlap Rate
10.0%	70.11%
20.0%	77.46%
50.0%	82.60%
60.0%	81.92%

Table 7: Dataset Statistics for Transductive Knowledge Graph Reasoning Datasets.

Dataset	Relation	Entity	Triplet		
			Train	Valid	Test
FB15k-237 [45]	237	14,541	272,115	17,535	20,466
WN18RR [46]	11	40,943	86,835	3,034	3,134
NELL-995 [61]	200	74,536	149,678	543	2,818
YAGO3-10 [62]	37	123,182	1,079,040	5,000	5,000

## C.2 Baseline details.

In this section, we explain the reasons for not comparing with some baseline methods on certain datasets. SimKGC [52] requires additional textual information as part of its input data. Since the public repository does not provide textual information for some datasets (e.g., NELL-995), comparisons on those datasets are not conducted. DRUM [50] and A\*Net [11] do not provide the specific parameters required to construct the inductive datasets as described in their papers. Therefore, they cannot be applied to certain datasets (e.g., NELL-995v1).

## D Experimental Details

### D.1 Dataset Statistics

We conduct experiments on four knowledge graph reasoning datasets, and the statistics of these datasets are summarized in Table 7. The specific dataset details are as follows:

- The FB15k-237 [45] dataset is a subset of FB15k [59]. Toutanova and Chen [45] pointed out that WN18 and FB15k have a test set leakage problem. Therefore, they extracted FB15k-237 from FB15k.
- The WN18RR [46] dataset is a subset of WN18 [59]. All inverse relations in the WN18 dataset were removed by Dettmers et al. [60] to obtain the WN18RR dataset.
- NELL-995 [61] is a refined subset of the NELL knowledge base, curated for multi-hop reasoning tasks by filtering out low-value relations and retaining only the top 200 most frequent ones.
- YAGO3-10 [62] is a subset of YAGO3, containing 123,182 entities and 37 relations, where most relations provide descriptions of people. Some relationships have a hierarchical structure such as *playsFor* or *actedIn*, while others induce logical patterns, like *isMarriedTo*.

Additionally, we perform experiments on three inductive knowledge graph reasoning datasets, each of which contains four different splits. The statistics of the inductive datasets are summarized in Table 8.

Table 8: Dataset Statistics for Inductive Knowledge Graph Reasoning Datasets. In each split, one needs to infer Query triplets based Fact triplets.

Dataset	Relation	Entity	Train			Valid			Test		
			Entity	Query	Fact	Entity	Query	Fact	Entity	Query	Fact
FB15k-237 [45]	180 (v1)	1,594	1,594	4,245	4,245	1,594	489	4,245	1,093	205	1,993
	200 (v2)	2,608	2,608	9,739	9,739	2,608	1,166	9,739	1,660	478	4,145
	215 (v3)	3,668	3,668	17,986	17,986	3,668	2,194	17,986	2,501	865	7,406
	219 (v4)	4,707	4,707	27,203	27,203	4,707	3,352	27,203	3,051	1,424	11,714
WN18RR [46]	9 (v1)	2,746	2,746	5,410	5,410	2,746	630	5,410	922	188	1,618
	10 (v2)	6,954	6,954	15,262	15,262	6,954	1,838	15,262	2,757	441	4,011
	9 (v3)	12,078	12,078	25,901	25,901	12,078	3,097	25,901	5,084	605	6,327
	9 (v4)	3,861	3,861	7,940	7,940	3,861	934	7,940	7,084	1,429	12,334
NELL-995 [61]	14 (v1)	3,103	3,103	4,687	4,687	3,103	414	4,687	225	100	833
	86 (v2)	2,564	2,564	15,262	8,219	2,564	922	8,219	2,086	476	4,586
	142 (v3)	4,647	4,647	16,393	16,393	4,647	1,851	16,393	3,566	809	8,048
	76 (v4)	2,092	2,092	7,546	7,546	2,092	876	7,546	2,795	7,073	731



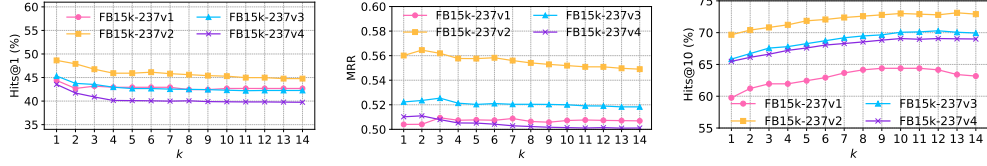


Figure 5: Effect of hyperparameter  $k$  on the performance metrics of KG reasoning for different datasets (inductive).

## D.2 Hyperparameters Setup

**Coarse-to-Fine reasoning model.** In the coarse-grained reasoning stage, we directly adopt existing models without any modifications to their original hyperparameter settings.

**Dual-Pathway fusion model.** For each dataset, we perform hyperparameter tuning on the validation set. We conduct grid search over the following hyperparameters:

- **Learning rate:**  $\{10^{-4}, 5 \times 10^{-4}, 10^{-3}, 5 \times 10^{-3}, 10^{-2}\}$
- **Weight decay:**  $\{10^{-5}, 10^{-4}\}$
- **Hidden dimension:**  $\{16, 32, 64, 128\}$
- **Negative sampling size:**  $\{128, 256, 512\}$
- **Message passing layers in input encoder:**  $\{1, 2, 3\}$
- **Message passing layers in local pathway:**  $\{1, 2, 3\}$
- **Transformer layers in global pathway:**  $\{1, 2, 3\}$

**Coarse-to-Fine Optimization.** In the coarse-to-fine optimization, two key hyperparameters are involved: the number of entities in the high-confidence subset  $k$ , and the decision threshold  $\Delta$ .

We analyze the impact of the hyper-parameter  $k$ , which denotes the number of entities in the high-score subset. We conduct experiments on the validation sets of all transductive datasets using our model. We set  $k$  to  $\{1, 2, 3, 4, 5, 6, 7, 8, 9, 10, 11, 12, 13, 14, 15\}$ . See Table 9. We ultimately select  $k = 7$  for WN18RR and  $k = 4$  for the other datasets, as these settings yield relatively high and stable results across three key metrics—MRR, Hits@1, and Hits@10—rather than optimizing a single metric in isolation. We also conduct the same experiments on 4 inductive datasets (As shown in Figure 5).

Additionally, We analyze the impact of the hyper-parameter, the decision threshold  $\Delta$ . We run experiments on all transductive datasets with our model. We set  $\Delta$  to  $\{0, 0.5, 1, 1.5, 2, 2.5, 3, 3.5, 4, 4.5, 5, 5.5, 6, 6.5, 7, 7.5, 8, 8.5, 9, 9.5, 10\}$ . For FB15k-237 and WN18RR, we set  $\Delta$  as 8 and set  $\Delta$  as 5 for NELL-995 and YAGO3-10.

**Computational Environment.** The experiments are conducted using Python 3.9.21, PyTorch 2.6.0, and CUDA 12.1, with an NVIDIA A100 80GB GPU.

## D.3 Random Initialization.

We run each model three times with different random seeds and report the mean results. We do not report the error bars because our model has very small errors with respect to random initialization. The standard deviations of the results are very small. For example, the standard deviations of MRR, H@1 and H@10 of DuetGraph are  $9.8 \times 10^{-7}$ ,  $5.6 \times 10^{-7}$  and  $1.95 \times 10^{-5}$  on FB15k-237 dataset, respectively. On WN18RR dataset, the standard deviations of MRR, H@1 and H@10 of DuetGraph are  $1.607 \times 10^{-6}$ ,  $7.77 \times 10^{-6}$  and  $8.94 \times 10^{-6}$ , respectively. On NELL-995 dataset, the standard deviations of MRR, H@1 and H@10 of DuetGraph are  $5.625 \times 10^{-7}$ ,  $1.0 \times 10^{-8}$  and  $1.89 \times 10^{-5}$ , respectively. On YAGO3-10 dataset, the standard deviations of MRR, H@1 and H@10 of DuetGraph are  $2.64 \times 10^{-6}$ ,  $4.3 \times 10^{-7}$  and  $2.5 \times 10^{-5}$ , respectively. This indicates that our model is not sensitive to the random initialization.

Table 9: The results on transductive knowledge graph reasoning datasets with different  $k$ .

Value	FB15k-237			WN18RR			NELL-995			YAGO3-10		
	MRR	H@1	H@10	MRR	H@1	H@10	MRR	H@1	H@10	MRR	H@1	H@10
1	0.455	37.7	61.6	0.602	55.0	70.4	0.592	54.6	68.1	0.638	58.3	74.2
2	0.457	37.0	61.9	0.599	53.6	70.6	0.594	54.6	68.2	0.636	57.0	74.4
3	0.456	36.4	62.3	0.595	52.4	70.9	0.592	54.1	68.4	0.634	56.5	74.6
4	0.456	36.1	62.8	0.593	52.2	71.2	0.592	54.1	68.5	0.632	56.1	74.9
5	0.454	35.8	63.0	0.591	52.0	71.4	0.593	54.1	68.7	0.631	55.9	75.2
6	0.452	35.5	63.4	0.589	51.9	71.5	0.593	54.1	69.0	0.629	55.7	75.4
7	0.452	35.4	63.9	0.589	51.8	71.7	0.594	54.2	69.3	0.628	55.5	75.6
8	0.451	35.4	64.2	0.588	51.7	71.9	0.593	54.1	69.5	0.627	55.4	75.8
9	0.451	35.4	64.6	0.588	51.7	72.1	0.594	54.2	69.8	0.626	55.3	75.9
10	0.450	35.3	65.1	0.587	51.6	72.4	0.594	54.2	70.0	0.626	55.3	76.2
11	0.450	35.3	65.2	0.587	51.5	72.1	0.595	54.1	70.1	0.625	55.2	76.2
12	0.450	35.3	65.2	0.584	51.0	72.1	0.593	53.9	70.0	0.624	55.1	76.2
13	0.449	35.2	65.1	0.583	50.9	72.2	0.592	53.9	69.9	0.624	55.0	76.1
14	0.449	35.2	65.0	0.583	50.9	72.1	0.592	53.9	69.9	0.623	55.0	76.0
15	0.447	35.0	64.9	0.582	50.9	72.0	0.591	53.8	69.8	0.623	54.9	75.8

## E Limitations and Broader Impacts

### E.1 Limitations

Although DuetGraph has demonstrated its effectiveness in improving reasoning performance on several public benchmarks, many challenges remain to be addressed. For instance, its black-box decision process poses challenges for domains such as biomedicine, where expert interpretability and traceability are essential. Future work may incorporate explainability modules along with interactive visualization tools to help users understand the reasoning process of the model, thereby improving its trustworthiness and applicability in real-world scenarios such as clinical diagnosis and drug discovery [63].

### E.2 Broader Impacts

DuetGraph is a framework for knowledge graph reasoning that offers strong support for predicting missing information in real-world social networks. And DuetGraph holds great potential for accelerating discovery in biomedical domains, such as drug repurposing and disease-gene association prediction.